Catalytic activities of non-noble metals for hydrogen generation from aqueous ammonia–borane at room temperature

Qiang Xu [*], Manish Chandra

National Institute of Advanced Industrial Science and Technology (AIST), 1-8-31 Midorigaoka, Ikeda, Osaka 563-8577, Japan

Abstract

We have studied catalytic performance of supported non-noble metals for hydrogen generation from aqueous NH_3BH_3 at room temperature. Among the tested non-noble metals, supported Co, Ni and Cu are the most catalytically active, with which hydrogen is released with an almost stoichiometric amount from aqueous NH_3BH_3, whereas supported Fe is catalytically inactive for this reaction. Support effects on the catalytic activity have been investigated by testing the hydrogen generation reaction in the presence of Co supported on γ-Al_2O_3, SiO_2 and C and it is found that the Co/C catalyst has higher activity. Activation energy for hydrogen generation from aqueous NH_3BH_3 in the presence of Co/γ-Al_2O_3 was measured to be $62\,kJ\,mol^{-1}$; this may correspond to the step of B−N bond breaking. Particle size, surface morphology and surface area of the supported metal catalysts were examined by X-ray diffraction (XRD), transmission electron microscope (TEM), energy dispersive X-ray (EDX) and BET experiments. It is found that with decreasing the particle size the activity of the supported catalyst is increased. The low-cost and high-performance supported non-noble metal catalysts may have high potential to find its application to the hydrogen generation for portable fuel cells.
© 2006 Elsevier B.V. All rights reserved.

Keywords: Cobalt; Nickel; Copper; Hydrogen generation; Catalyst; Ammonia–borane

1. Introduction

The fuel cell concept, mostly studied and developed for large energy systems for many years, is now more and more considered for small portable power sources. It is anticipated that chemical hydrides will play an important role in hydrogen-based portable energy systems. Recently much attention has been paid to the hydrolysis of base stabilized $NaBH_4$, which shows a number of advantages as a hydrogen source for portable applications [1–7]. $NaBH_4$ is a good candidate for hydrogen generation for portable device under ambient conditions, whereas it requires a highly basic NaOH solution to avoid self-hydrolysis in water. Hydrogen generation by the hydrolysis of $LiBH_4$ has also been reported [8].

The ammonia–borane complex, NH_3BH_3, which contains 19.6 wt.% hydrogen and is stable under ordinary storage conditions, possesses high potential for hydrogen generation for portable devices. There have already been a number of reports on the H_2 release from NH_3BH_3. The pyrolysis of NH_3BH_3 in the pure form [9–12], infused in nanoporous silica [13] and doped with platinum catalyst [14] has been widely investigated. A catalytic dehydrocoupling route to derivatives of aminoborane, $(NH_2BH_2)_3$, and borazine, $(NHBH)_3$, from either primary or secondary amine–borane adducts has been developed using late transition-metal catalysts [15–17]. The rhodium catalyzed dehydrogenation of dimethylaminoboranes has also been studied [18]. Dehydrogenation of ammonia–borane in ionic liquid at $95\,^{\circ}C$ releases 1.6 equivalent of H_2 along with traces of borazine in 22 h [19].

Ammonia–borane has high solubility in water [12,20,21], while, unlike $NaBH_4$ [22] which undergoes self-hydrolysis without high-concentration NaOH solution, NH_3BH_3 is highly stable in water as observed in the previous ^{11}B NMR measurements [23,24]. Recently we have reported that with noble metal catalysts NH_3BH_3 undergoes dissociation and hydrolysis with a very high kinetics to release hydrogen with $H_2/NH_3BH_3 = 3.0$ [23]. It has been found that solid acids, such as cation-exchange resins and zeolites, also exhibit catalytic activity to this reaction

* Corresponding author. Tel.: +81 72 751 9562; fax: +81 72 751 9629.
E-mail address: q.xu@aist.go.jp (Q. Xu).

[24]. For practical use, the development of low-cost and highly efficient catalysts is desired. Keeping this in view we tested the catalytic activity of non-noble metals such as Fe, Co, Ni and Cu supported on various supports, viz. γ-Al$_2$O$_3$, SiO$_2$ and C, which are low-cost in comparison with the noble metal catalysts, for hydrogen generation from aqueous NH$_3$BH$_3$. It is found that the supported Co, Ni and Cu catalysts show high activities to the hydrolysis of NH$_3$BH$_3$ to release hydrogen up to H$_2$/NH$_3$BH$_3$ = 3.0, which is pure enough to be used directly to PEM fuel cells.

2. Experimental

2.1. Preparation of catalysts

Supported metal catalysts used in this study were prepared by a conventional impregnation method. γ-Al$_2$O$_3$ (aluminium oxide, specific surface area = 43 m^2 g^{-1}, Aldrich), SiO$_2$ (fumed silica, specific surface area = 390 m^2 g^{-1}, Aldrich), VULCAN$^{\circledR}$ carbon (VULCAN XC-72R, specific surface area = 240 m^2 g^{-1}, Cabot Corp., USA) were used as the catalytic supports. For preparing γ-Al$_2$O$_3$ and SiO$_2$ supported catalysts, impregnation was performed by stirring the supports with known amounts of aqueous solutions of Fe(NO$_3$)$_3$·xH$_2$O, Cu(NO$_3$)$_2$·xH$_2$O (Aldrich), Co(NO$_3$)$_2$·6H$_2$O (High Purity Chemicals) and Ni(NO$_3$)$_2$·6H$_2$O (Wako Chemicals), respectively, at 363 K for 12–16 h. The solvent was evaporated to dryness at 363 K. The Fe, Co, Ni and Cu samples were calcined in air for 5 h at 873 K. After purging argon in the fixed bed stainless steel reactor containing the calcined samples, a continuous H$_2$ gas flow was introduced to the sample at the rate of 50 ml min^{-1} at 773 K for 5 h for reduction. For preparing the VULCAN$^{\circledR}$ carbon supported cobalt catalyst, impregnation was performed by ultrasonicating the mixture of Co(NO$_3$)$_2$ dissolved in methanol and VULCAN$^{\circledR}$ carbon for 30 min at room temperature. The ultrasonicated sample was dried at 363 K for 12 h and then the dried sample was reduced by a continuous H$_2$ gas flow at a rate of 150 ml min^{-1} at 573 K for 5 h in a similar way. After reduction the catalysts were stored in an argon atmosphere until being used for hydrogen generation.

2.2. Characterization of catalysts

The Co/γ-Al$_2$O$_3$, Ni/γ-Al$_2$O$_3$ and Cu/γ-Al$_2$O$_3$ catalysts were characterized by powder X-ray diffraction (XRD) using a Cu Kα X-ray source (40 kV, 100 mA) on a Rigaku RINT-2000 diffractometer. The catalysts were packed on a glass substrate and covered by an adhesive tape on the surface to minimize the samples exposure to oxygen and moisture during the measurement. The average crystallite sizes of metals (thickness of crystal in direction perpendicular to the lattice plane of (1 1 0) for Fe and of (1 1 1) for others) were determined by the Scherrer's formula (1) and the surface areas of catalysts were calculated using Eq. (2)

$$d = \frac{k\lambda}{\beta \cos\theta} \tag{1}$$

$$S = \frac{6000}{\rho d} \tag{2}$$

where d is the average particle sizes (nm), S the surface area of metals (m^2 g^{-1}), β the half width in radians, λ the wavelength (0.154 nm), θ the Bragg angle ($^\circ$), k the Scherrer's constant of 0.9 and ρ is the density of metal. Densities of Co, Ni, Cu and Fe are 8.90, 8.90, 8.92 and 7.86 m^2 g^{-1}, respectively [25]. Table 1 lists calculated average particle sizes and surface areas of the metals obtained by XRD data for Co/C, Co/SiO$_2$, Co/γ-Al$_2$O$_3$, Ni/γ-Al$_2$O$_3$, Cu/γ-Al$_2$O$_3$ and Fe/γ-Al$_2$O$_3$ catalysts on the basis of the strongest diffraction peaks of Co(1 1 1), Ni(1 1 1), Cu(1 1 1) and Fe(1 1 0), respectively, shown in Fig. 1.

The morphology of the catalysts was observed using a Tecnai G^2 20 Twin (FEI) transmission electron microscope (TEM) operating with an acceleration voltage of 200 kV, which was equipped with a CCD camera (Gatan Image Filter) and an energy dispersive X-ray detector (EDAX). For preparing the TEM samples catalysts were dispersed in ethanol followed by ultrasonicating for 10 min. One drop of the suspension was placed on the TEM grid and dried for 30 min.

The textural data of catalysts were measured by N$_2$ adsorption at liquid N$_2$ temperature with a micromeritics ASAP 2010

Table 1
Characteristics of supports and catalysts tested for the hydrogen generation reaction

Catalysts	Metal content (wt.%)	BET surface area (m^2 g^{-1})	Average particle size by XRD[a] (nm)	Surface area of metal[b] (m^2 g^{-1})
γ-Al$_2$O$_3$	–	43	–	–
SiO$_2$[c]	–	390	–	–
C[d]	–	240	–	–
Co/γ-Al$_2$O$_3$	10.0	37	13	52
Co/SiO$_2$	10.0	310	12	57
Co/C	10.0	210	2.5	270
Ni/γ-Al$_2$O$_3$	10.0	37	3.8	180
Cu/γ-Al$_2$O$_3$	10.0	34	17	39
Fe/γ-Al$_2$O$_3$	10.0	36	16	47

[a] Calculated on the basis of the width of the strongest X-ray diffraction peak (1 1 1) for Co, Ni and Cu catalysts, and (1 1 0) for Fe catalysts.
[b] Calculated from the average particle size.
[c] Fumed SiO$_2$.
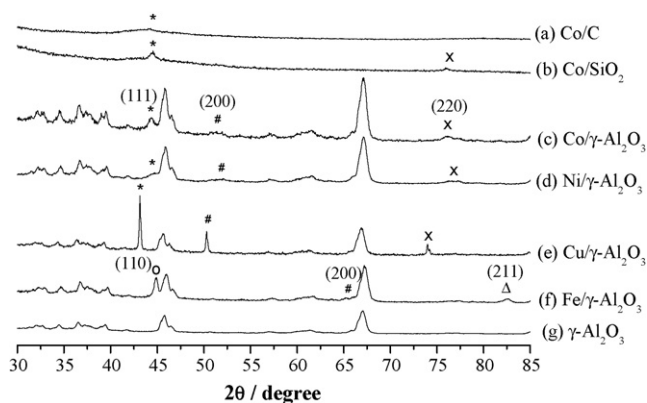[d] VULCAN$^{\circledR}$ carbon.

Fig. 1. Powder X-ray diffraction profiles for the supported Co, Ni and Cu catalysts.

BET analyzer. Before the analysis the samples were outgassed at 300 °C under vacuum for 4 h.

2.3. Hydrogen generation

A commercial ammonia–borane complex (Tech. 90%, Aldrich) was used as purchased. Reaction apparatus for measuring the hydrogen generation rate from the aqueous NH_3BH_3 solution is similar to that previously reported [23,24]. In general, the hydrolysis reactions of aqueous NH_3BH_3 with prepared catalysts were carried out at room temperature. A weighed catalyst was placed in the three-necked round-bottom flask (50 ml) and the reaction was started by stirring the mixture of the catalyst and the aqueous NH_3BH_3 solution added from the addition funnel, and the evolution of gas was monitored using the gas buret to an accuracy of ±0.5 ml. A water jacket was used to keep the solution temperature constant within the range of the set value of ±1.0 °C. For obtaining the activation energy, we carried out the hydrogen generation reaction at 20, 25, 30 and 40 °C. The ^{11}B NMR and measurements were performed using a JEOL JNM-AL400 spectrometer operating at 128.15 MHz and the MS measurements on a Balzers Prisma QMS 200 mass spectrometer as described previously [24].

3. Results and discussion

Our previous investigations have shown the metal-catalyzed dissociation and hydrolysis of NH_3BH_3 at room temperature in the presence of noble metal [23] and acid catalysts [24]. Among these catalysts Pt catalysts were found to be the most active, which release stoichiometric amount of H_2 from aqueous NH_3BH_3 ($H_2/NH_3BH_3 = 3.0$). Our present effort has been devoted to obtain the stoichiometric amount of H_2 from NH_3BH_3 with fast kinetics in the presence of less costly non-noble metal catalysts.

Fig. 1 shows the X-ray diffraction profiles of the Co/C, Co/SiO_2, Co/γ-Al_2O_3, Ni/γ-Al_2O_3, Cu/γ-Al_2O_3 and Fe/γ-Al_2O_3 catalysts. For comparison, the XRD profile for the γ-Al_2O_3 support is also included (Fig. 1g). As shown in Fig. 1, the γ-Al_2O_3 support is crystalline, while the VULCAN® carbon

and SiO_2 supports are amorphous. A broad (1 1 1) diffraction peak was observed for the Co/C catalysts, indicating a small average Co particle size. The profiles of γ-Al_2O_3 supported metals (Fig. 1c–e) clearly indicate the three characteristic peaks of the face centered cubic crystalline Co, Ni and Cu, namely (1 1 1), (2 0 0) and (2 2 0). The profile of the Fe/γ-Al_2O_3 catalyst (Fig. 1f) show the characteristic peaks of the body centered cubic crystalline Fe, namely (1 1 0), (2 0 0) and (2 1 1). The observed XRD profiles indicate the formation of Co^0, Ni^0, Cu^0 and Fe^0 (Co^0: $2\theta = 44.216°$, $51.522°$, $75.853°$ JCPDS # 15-0806; Ni^0: $2\theta = 44.507°$, $51.846°$, $76.370°$ JCPDS # 04-0850; Cu^0: $2\theta = 43.297°$, $50.433°$, $74.130°$ JCPDS # 04-0836; Fe^0: $2\theta = 44.673°$, $65.021°$, $82.333°$ JCPDS # 06-0696). Co/SiO_2 and Co/γ-Al_2O_3 show a similar diffraction pattern for Co particles. Table 1 lists average particle sizes for the catalysts, calculated on the basis of the strongest diffraction peak of Co(1 1 1), Ni(1 1 1) and Cu(1 1 1). The calculated metal particle sizes are 13, 12, 2.5, 3.8, 17 and 16 nm for the Co/γ-Al_2O_3, Co/SiO_2, Co/C, Ni/γ-Al_2O_3, Cu/γ-Al_2O_3 and Fe/γ-Al_2O_3 catalysts, corresponding to surface areas of 52, 57, 270, 180, 39 and 47 $m^2 g^{-1}$, respectively.

The morphology of catalysts was examined using TEM and energy dispersive X-ray (EDX) spectrometry. The Co/γ-Al_2O_3 catalyst gives a TEM image of a low contrast, with which we cannot distinguish between the two components. To identify the presence of Co on the γ-Al_2O_3 support we have carried out EDX experiments. Fig. 2a–c shows high angle annular dark field (HAADF) image and EDX spectra of the surface of the γ-Al_2O_3 support and Co deposited on it. The EDX analyses indicate the presence of Co on the large alumina particle. The EDX spectrum for point 1 marked in Fig. 2a exhibits Kα peaks corresponding to Al, Co and Cu elements at 1.48, 6.93 and 8.04 keV, respectively (Fig. 2b), indicating the presence of Co. The Cu signal at 8.04 keV is from the TEM grid. Another EDX spectrum (Fig. 2c) for point 2 marked in Fig. 2a exhibits Kα peak at 1.48 and 8.04 keV corresponding to Al and Cu, respectively. The absence of Co peak in Fig. 2c supports the dispersion of cobalt on alumina particles. The HRTEM image of Ni/γ-Al_2O_3 catalyst shows dark Ni crystalline spots embedded on γ-Al_2O_3 (Fig. 3a and b). The γ-Al_2O_3 support and dispersed Ni metal particles are almost spherical and crystalline. The average Ni particle size appeared in TEM is about 6 nm. It is close to the value obtained from the XRD data (Table 1). The Cu/γ-Al_2O_3 catalyst (figure not shown in this paper) exhibits a TEM image of low contrast, similarly to that of the Co/γ-Al_2O_3 catalyst. Fig. 4 exhibits the HAADF image and EDX spectrum of Cu/γ-Al_2O_3. The EDX spectrum for the selected area in Fig. 4a indicates the presence of Kα peaks corresponding to Al, Cu and Mo elements at 1.48, 8.04 and 17.48 keV, respectively. The peak at 17.48 keV is due to the Mo TEM grid.

The specific surface areas of all the catalysts determined by using the BET method, is summarized in Table 1. There are only small changes in the surface area with loading metals to the γ-Al_2O_3, SiO_2 and VULCAN® carbon supports.

It has been reported that the ^{11}B resonance of aqueous NH_3BH_3 remains unchanged for more than 80 days under argon atmosphere, indicating the high stability of NH_3BH_3 in
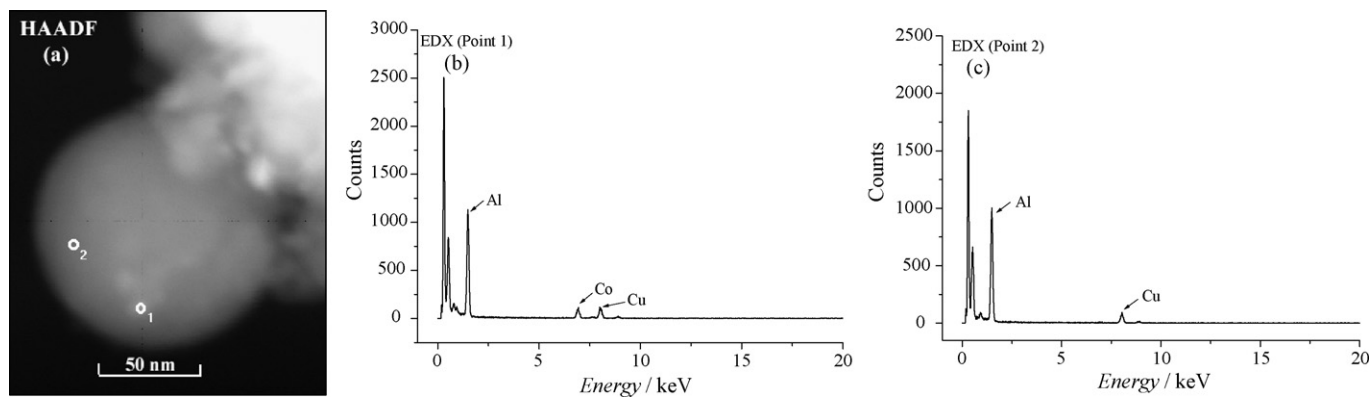
Fig. 2. (a) HAADF image of the Co/γ-Al$_2$O$_3$ (10 wt.%) catalyst and the corresponding EDX spectra at (b) point 1 and (c) point 2 in (a). The Cu signal in (b) and (c) is due to the TEM grid.
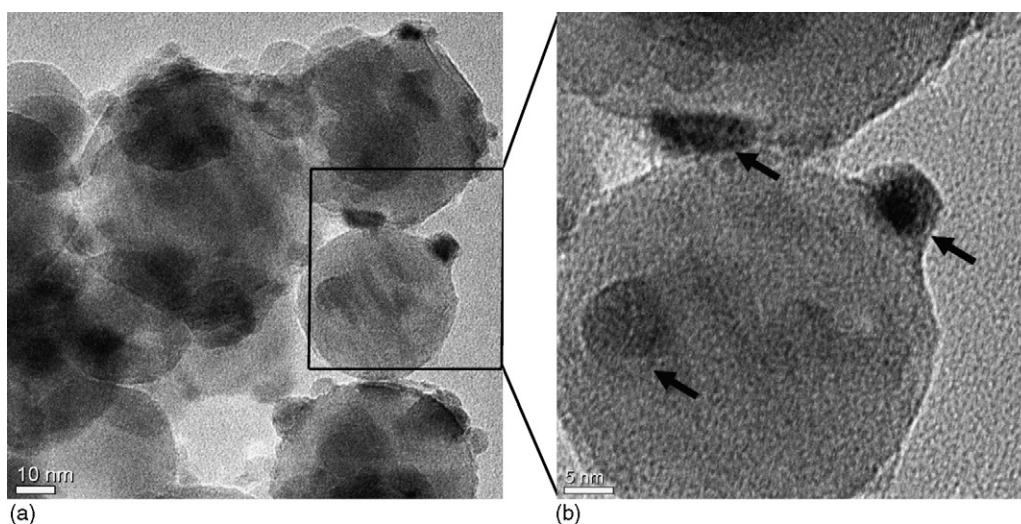

Fig. 3. HRTEM image of Ni/γ-Al$_2$O$_3$ (10 wt.%) catalyst. Arrow indicates nickel particles over large γ-Al$_2$O$_3$ particles.

water [24]. It is found that the addition of catalytic amounts of non-noble metal catalysts such as Co/γ-Al$_2$O$_3$, Co/SiO$_2$, Co/C, Ni/γ-Al$_2$O$_3$ and Cu/γ-Al$_2$O$_3$ leads to vigorous release of pure hydrogen, which has been identified by mass spectrometry. No significant amount of impurity NH$_3$ was observed in the MS

analysis of the released hydrogen gas. The [11]B resonance at −23.9 ppm for aqueous NH$_3$BH$_3$ [23,24,26–29] disappears after the reaction is completed, giving a low field-shifted single [11]B resonance at 8.6 ppm. The observation indicates that the reaction with non-noble metal catalysts is the same as that with the
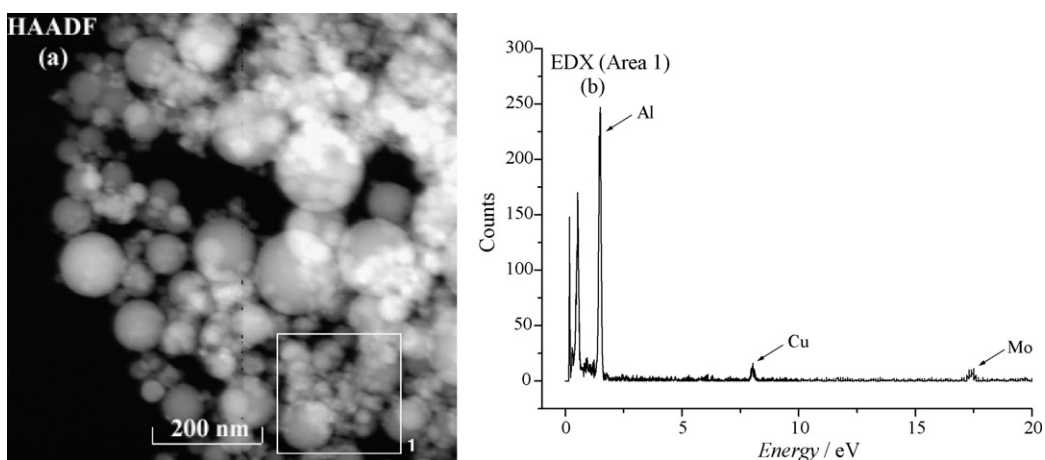
Fig. 4. (a) HAADF image of the Cu/γ-Al$_2$O$_3$ (10 wt.%) catalyst and the corresponding EDX spectrum of area 1 in (a). The Mo signal in (b) is due to the TEM grid.
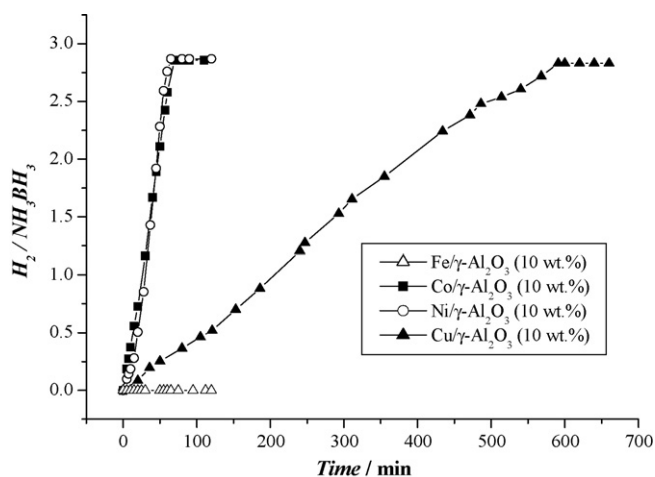
Fig. 5. Hydrogen generation from aqueous NH_3BH_3 (1 wt.%, 10 ml) in the presence of γ-Al_2O_3 supported catalysts (metal/NH_3BH_3 = 0.018).

Fig. 6. Hydrogen generation from aqueous NH_3BH_3 (1 wt.%, 10 ml) in the presence of Co/γ-Al_2O_3 (10 wt.%), Co/SiO_2 (10 wt.%) and Co/C (10 wt.%) (metal/NH_3BH_3 = 0.018).

noble metal catalysts (Eq. (3)) [23].

$$NH_3BH_3 + 2H_2O \xrightarrow[\text{r.t.}]{\text{Metal}} NH_4^+ + BO_2^- + 3H_2 \qquad (3)$$
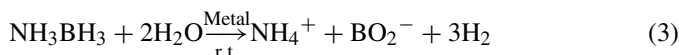
Fig. 5 shows the hydrogen generation with time from aqueous NH_3BH_3 in the presence of the γ-Al_2O_3 supported Fe, Co, Ni and Cu catalysts with the metal contents normalized to the same (M/NH_3BH_3 = 0.018). The reaction rate significantly depends on the metal catalysts employed. It has been confirmed that the γ-Al_2O_3 support used is inactive to this reaction. As shown in Fig. 5, the Co/γ-Al_2O_3 and Ni/γ-Al_2O_3 catalysts are almost equally active, exhibiting the hydrogen release of H_2/NH_3BH_3 = 2.86 and 2.87 in 70 and 65 min, respectively. The Cu/γ-Al_2O_3 catalyst is less active, releasing hydrogen of H_2/NH_3BH_3 = 2.83 in 590 min. The Fe/γ-Al_2O_3 catalyst is inactive, with which the [11]B resonance at −23.9 ppm due to the starting material NH_3BH_3 remains unchanged after stirring the solution for 125 min. The higher activity of Co/γ-Al_2O_3 and Ni/γ-Al_2O_3 in comparison to Cu/γ-Al_2O_3 may be due to the smaller particle sizes of the Co/γ-Al_2O_3 and Ni/γ-Al_2O_3 catalysts as described above.

We have tested the catalytic activities of Co on different supports with the Co content kept unchanged (10 wt.% Co/support, Co/NH_3BH_3 = 0.018). As shown in Fig. 6, the hydrogen generation rates from aqueous NH_3BH_3 are almost the same in the presence of Co/γ-Al_2O_3 and Co/SiO_2, whereas the Co/C catalyst exhibits higher catalytic activity. As listed in Table 1, the Co/γ-Al_2O_3 and Co/SiO_2 catalysts have almost the same metal particle sizes and surface areas, while the Co/C catalyst has a rather smaller particle size and a larger surface area. It is noted that commercial cobalt powders with particle sizes in microns are not active to this reaction as previously reported [23]. The observations indicate that the higher dispersion and smaller particle size of Co on the support correspond to higher catalytic activity. Although the particle size is an important factor for the catalytic activity as observed for the supported Co catalysts, it is worthy to note that the nanoparticles of Fe are not active to the present reaction.
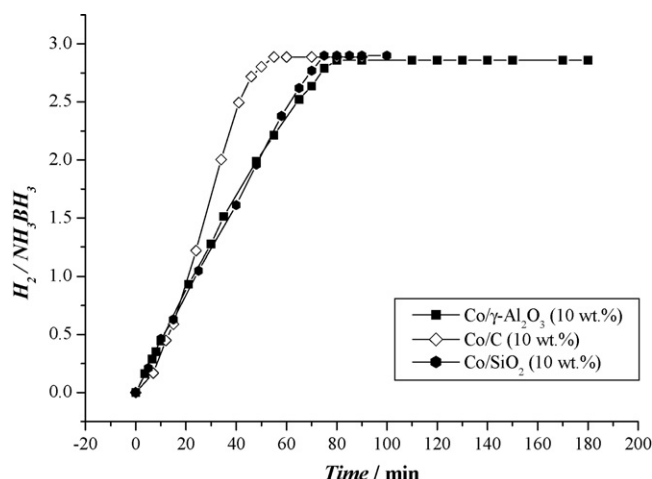
At 25 °C, the standard-state enthalpy change for Eq. (3) can be calculated to be −156 kJ mol^{-1} from the standard enthalpies of −178 kJ mol^{-1} (NH_3BH_3), −572 kJ mol^{-1} (2H_2O), −133 kJ mol^{-1} (NH_4^+), −772 kJ mol^{-1} (BO_2^-) and 0 (3H_2) [25] and this reaction is exothermic. In comparison, the standard-state enthalpy change for the hydrogen generation reaction of sodium borohydride $NaBH_4 + 2H_2O \rightarrow NaBO_2 + 4H_2$ is −217 kJ mol^{-1} [3].

Generally, the chemical reaction rate increases with the reaction temperature. For determining the activation energy, we measured the temperature dependence of hydrogen generation rate using 1 wt.% aqueous NH_3BH_3 with the 10 wt.% Co/γ-Al_2O_3 catalysts (Co/NH_3BH_3 = 0.018) in the temperature range of 20–40 °C (Fig. 7a). Volume of H_2 generated by the Co/γ-Al_2O_3 catalyzed hydrolysis of NH_3BH_3 increased linearly with time.

$$-\frac{1}{3}\frac{d[NH_3BH_3]}{dt} = \frac{d[H_2]}{dt} = k \qquad (4)$$

Under our experimental conditions, the reaction rate constant, k, is constant for a given temperature, implying zero order kinetics for the NH_3BH_3 hydrolysis reaction. This suggests that the hydrogen generation rate is controlled within a surface reaction.

The reaction rate equation can be written as follows:

$$k = k_0 \exp^{-E/RT} \qquad (5)$$

where k_0 is the reaction constant (ml min^{-1}), E the activation energy for the reaction, R the gas constant and T is the reaction temperature. Following the above mentioned equation, $\log k$ versus $1/T$ was plotted in Fig. 7b. The activation energy for the hydrogen generation reaction from the Co/γ-Al_2O_3 catalyzed hydrolysis reaction is then calculated to be 62 kJ mol^{-1} from the slope of Fig. 7b. For comparison, in case of hydrogen generation from aqueous $NaBH_4$ the activation energy is 69 kJ mol^{-1} for the Co-B catalyst [5] and 75 kJ mol^{-1} for the Co-only catalyst [30].

The role of the non-noble metal catalysts in the hydrogen generation reaction is of particular interest. For the present
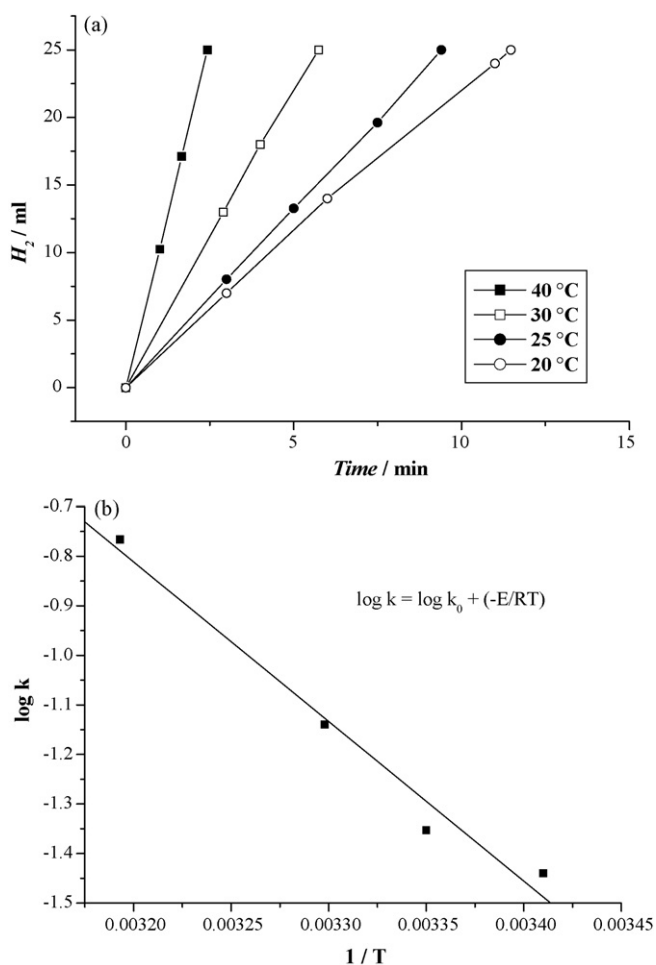
Fig. 7. (a) Hydrogen generation from aqueous NH_3BH_3 (1 wt.%, 10 ml) in the presence of Co/γ-Al_2O_3 (10 wt.%) at 20, 25, 30 and 40 °C and (b) the log k vs. $1/T$ plot calculated from (a) ($Co/NH_3BH_3 = 0.018$). Calculated activation energy is 62 kJ mol^{-1}.

metal-catalyzed reaction, there seems no doubt that the activation process takes place on the metal catalyst surfaces, as suggested by the zero order kinetics (Fig. 7). As one of plausible mechanisms, it is reasonable to consider that there should be interactions between the NH_3BH_3 molecule and the metal particle surface to form activated complex species (Scheme 1), which is most likely the rate-determining step, to which attack by a H_2O molecule readily leads to concerted dissociation of the B–N bonding and hydrolysis of the resulting BH_3 intermediate to produce the borate ion along with the H_2 release. Interestingly, in the absence of H_2O, dehydrocoupling between
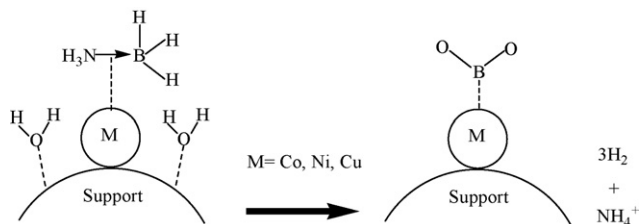
Scheme 1. Schematic representation of hydrolysis of NH_3BH_3 in the presence of supported metal catalysts.

NH_3BH_3 molecules to form new B–N bonds occurs, probably via a closely related intermediate, on the metal surface [15–17].

In the present NH_3BH_3 system, 0.195 g of hydrogen is liberated per 1 g of the NH_3BH_3. In comparison, 0.084 g of hydrogen per 1 g of NaH, 0.213 g of hydrogen per 1 g of $NaBH_4$ and 0.254 g of hydrogen per 1 g of LiH are released in the respective hydrolysis reactions under appropriate conditions [3]. We can analyze the feasibility of using the chemical hydrides by hydrolysis as potential H_2 source for fuel cell applications. The generation of 1 g H_2 s^{-1} corresponds to 96.5 kA × 0.7 = 68 kW, assuming a standard PEM fuel cell operates at 0.7 V [3]. The amounts of NH_3BH_3, NaH, $NaBH_4$ and LiH needed are 0.27, 0.63, 0.25 and 0.21 kg, respectively, for supplying hydrogen to such a PEMFC system producing 1 kW of electric power for 1 h.

4. Conclusions

In this paper we have presented for the first time the hydrolysis of NH_3BH_3 in the presence of supported non-noble metal catalysts such as Co, Ni and Cu which produces pure hydrogen of nearly stoichiometric amount ($H_2/NH_3BH_3 = 3.0$) with fast kinetics at room temperature. The low-cost and high-performance supported non-noble metal catalysts have high potential to find its application to the hydrogen generation for portable fuel cells.

Acknowledgements

References

[1] S.C. Amendola, S.L. Sharp-Goldman, M.S. Janjua, M.T. Kelly, P.J. Petillo, M. Binder, J. Power Sources 85 (2000) 186.
[2] S. Suda, U.S. Patent, US 6,358,488 B1 (2002).
[3] Y. Kojima, K.I. Suzuki, K. Fukumoto, M. Sasaki, T. Yamamoto, Y. Kawai, H. Hayashi, Int. J. Hydrogen Energy 27 (2002) 1029.
[4] D. Hua, Y. Hanxi, A. Xinping, C. Chuansin, Int. J. Hydrogen Energy 28 (2003) 1095.
[5] S.U. Jeong, R.K. Kim, E.A. Cho, H.-J. Kim, S.-W. Nam, I.-H. Oh, S.-A. Hong, S.H. Kim, J. Power Sources 144 (2005) 129.
[6] S.C. Amendola, S.L. Sharp-Goldman, M.S. Janjua, N.C. Spencer, M.T. Kelly, P.J. Petillo, M. Binder, Int. J. Hydrogen Energy 25 (2000) 969.
[7] Z.P. Li, B.H. Liu, K. Arai, S. Suda, J. Electrochem. Soc. 150 (2003) A868.
[8] Y. Kojima, Y. Kawai, M. Kimbara, H. Nakanishi, S. Matsumoto, Int. J. Hydrogen Energy 29 (2004) 1213.
[9] J.S. Wang, R.A. Geanangel, Inorg. Chim. Acta 148 (1988) 185.
[10] G. Wolf, J. Baumann, F. Baitalow, F.P. Hoffmann, Thermochim. Acta 343 (2000) 19.
[11] J. Baumann, F. Baitalow, G. Wolf, Thermochim. Acta 430 (2005) 9.
[12] A. T-Raissi, Proceedings of the 2002. U.S. DOE Hydrogen Program Review, http://www.eere.energy.gov/hydrogenandfuelcells/pdfs/32405b15.pdf.

[13] A. Gutowska, L. Li, Y. Shin, C.M. Wang, X.S. Li, J.C. Linehan, R.S. Smith, B.D. Kay, B. Schmid, W. Shaw, M. Gutowski, T. Autrey, Angew. Chem. Int. Ed. 44 (2005) 3578.

[14] S.D. Benedetto, M. Carewska, C. Cento, P. Gislon, M. Pasquali, S. Scaccia, P.P. Prosini, Thermochim. Acta 441 (2006) 184.

[15] C.A. Jaska, K. Temple, A.J. Lough, I. Manners, Chem. Commun. (2001) 962.

[16] C.A. Jaska, K. Temple, A.J. Lough, I. Manners, J. Am. Chem. Soc. 125 (2003) 9424.

[17] C.A. Jaska, I. Manners, J. Am. Chem. Soc. 126 (2004) 9776.

[18] Y. Chen, J.L. Fulton, J.C. Linehan, T. Autrey, J. Am. Chem. Soc. 127 (2005) 3254.

[19] M.E. Bluhm, M.G. Bradley, R. Butterick III, U. Kusari, L.G. Sneddon, J. Am. Chem. Soc. 128 (2006) 7748.

[20] V.P. Sorokin, B.I. Vesnina, N.S. Klimova, Zh. Neorg. Khim. 66 (1963) 8.

[21] P.A. Storozhenko, R.A. Svitsyn, V.A. Ketsko, A.K. Buryak, A.V. Ul'yanov, Russ. J. Inorg. Chem. 50 (2005) 980.

[22] H.I. Schlesinger, H.C. Brown, A.E. Finholt, J.R. Gilbreath, H.R. Hoekstra, E.K. Hyde, J. Am. Chem. Soc. 75 (1953) 215.

[23] M. Chandra, Q. Xu, J. Power Sources 156 (2006) 190.

[24] M. Chandra, Q. Xu, J. Power Sources 159 (2006) 855.

[25] R.C. Weast, M.J. Astle, W.H. Beyer (Eds.), CRC Handbook of Chemistry and Physics, 67th ed., CRC Press, Florida, 1986/1987.

[26] D.F. Gaines, R. Schaeffer, J. Am. Chem. Soc. 86 (1964) 1505.

[27] C.W. Heitsch, Inorg. Chem. 4 (1965) 1019.

[28] B.F. Spielvogel, J.M. Purser, J. Am. Chem. Soc. 89 (1967) 5294.

[29] J.M. Purser, B.F. Spielvogel, Inorg. Chem. 7 (1968) 2156.

[30] C.M. Kaufman, B. Sen, J. Chem. Soc., Dalton Trans. (1985) 307.